Dynamic Behavior of Pb(II) and Cr(III) Biosorption onto Dead Anaerobic Biomass in Fixed-Bed Column, Single and Binary Systems

Abbas Hameed Sulaymon
Professor
College of Engineering
University of Baghdad
inas@yahoo.com

Shahlaa Esmail Ebrahim
Assistant Professor
College of Engineering
University of Baghdad
shahlaaaga@yahoo.com

Mohanad Jasim Mohammed Ridha
Instructor
College of Engineering
University of Baghdad
muhannadenviro@yahoo.com

ABSTRACT

The biosorption of lead (II) and chromium (III) onto dead anaerobic biomass (DAB) in single and binary systems has been studied using fixed bed adsorber. A general rate multi- component model (GRM) has been utilized to predict the fixed bed breakthrough curves for single and dual-component system. This model considers both external and internal mass transfer resistances as well as axial dispersion with non-liner multi-component isotherm (Langmuir model). The effects of important parameters, such as flow rate, initial concentration and bed height on the behavior of breakthrough curves have been studied. The equilibrium isotherm model parameters such as maximum uptake capacities for lead (II) and chromium (III) were found to be 35.12 and 23.84 mg g^{-1} respectively. While pore diffusion coefficients (D_p) were obtained to be 7.23×10^{-11} and 3.15×10^{-11} m^2 s^{-1} for lead (II) and chromium (III) respectively from batch experiments. The results show that the general rate model was found correct for describing the biosorption process of the dynamic behavior of the DAB adsorber column.

Key words: biosorption, DAB, lead (II), chromium (III), GRM, fixed bed, pore diffusion

السلوك الديناميكي من الرصاص (II) والكروم (III) الامتزاز الحيوي على الكتلة اللاهوائية الحيوية الميتة في عمود ثابت الكتلة، نظام مفرد و ثنائي

عباس حميد سليمون
استاذ
كلية الهندسة
جامعة بغداد

ا.م.د. شهلاء اسماعيل ابراهيم
استاذ مساعد
كلية الهندسة
جامعة بغداد

م.د. مهند جاسم محمد وضا
مدرس
كلية الهندسة
جامعة بغداد

الخلاصة

تم دراسة الامتزاز الحيوي لايونات كل من االرصاص (II) والكروم (III) على الكتلة الحيوية اللاهوائية الميتة (DAB) في نظام مفرد وثنائي وباستخدام نظام الكتلة الثابتة الممتزة. وقد استخدم النموذج العام المتعدد العناصر (GRM) للتنبؤ بمنحنيات اختراق نظام الكتلة الثابتة الممتزة المفرد والثنائي. وقد تم الاخذ بنظر الاعتبار في هذا النموذج كل من مقاومة نقل المادة على الاسطح الخارجية والداخلية للمادة الممتزة، فضلا عن التشتت والانتشار المحوري خلال الانتقال داخل العمود الحيوي مع موديل متعدد المكونات (Langmuir mode). وقد تم دراسة تاثير المتغيرات، مثل معدل التدفق، وتركيز وارتفاع المادة الممتزة داخل العمود على سلوك منحنيات الاختراق لتركيز معين. ومن تجارب الدفعة الواحدة تم الحصول على ثوابت نموذج الاتزان حيث وجد ان اعظم امتزاز كان 35.12 و23.84 mg g^{-1} لكل من ايونات الرصاص(II) و الكروم(III) على التوالي. ومعاملات الانتشار المسامي (D_P) كانت 7.23×10^{-11} و 5×10^{-11} m^2s^{-1} لكل من ايونات الرصاص(II) و الكروم(III) على التوالي. وأظهرت النتائج أن النموذج المعدل العام صحيح لوصف عملية الامتزاز الحيوي من السلوك الديناميكي.

الكلمات الرئيسية : الامتزاز الحيوي، الكتلة اللاهوائية الميتة، والرصاص (II)، الكروم (III)، النموذج العام المتعدد العناصر عمود الكتلة الثابتة، الانتشار المسامي

1. INTRODUCTION

Metallic species mobilized and released into the environment by the technological activities of humans tend to persist indefinitely, circulating and eventually accumulating throughout the food chain, thus posing a serious threat to the environment, animals, and humans. It is essential to realize that the metal is only "removed" from the solution when it is appropriately immobilized **Sekomo et al., 2011**. The continuous use of heavy metals in industrial applications with the production of contaminated wastewaters is a serious environmental problem these biomass types serve as a basis for newly developed metal biosorption processes foreseen particularly as a very competitive mean for the detoxification of metal-bearing industrial effluents **Van et al., 2006**. Only within the past decade has the potential of metal biosorption by biomass materials been well established. For economic reasons, biomass produced as a waste byproduct of large-scale industrial could be used as biosorbents **Prasad et al., 2008**. Lead (II) has been found together with other compounds including Chromium (III) at high concentrations in a number of contaminated sites **Naseem** and **Tahir, 2001**. Lead (II) and Chromium (III) are released from industrial sources such as the iron-steel, petroleum, wood preserving chemicals dye and pigment **Prasad et al., 2008**.

The use of natural biomass as adsorbent will involve the same concept of separation as in adsorption which is termed as biosorption **Fiol et al., 2004**. Biosorption is a well-established and powerful technique for treating domestic and industrial effluents **Sulaymon et al., 2012 b**. DAB is the new and effectively used adsorbent. Biosorbent for the removal of metals/dyes mainly come under the following categories: bacteria, fungi, algae, industrial wastes, agricultural wastes and other polysaccharide materials. In general, all types of biomaterials have shown good biosorption capacities towards all types of metal ions **Vijayaraghavan** and **Yun, 2008**. The surface chemistry of biomass and the chemical characteristics of adsorbate, such as polarity, ionic nature, functional groups, and solubility, determine the nature of bonding mechanisms as well as the extent and strength of adsorption **Sulaymon** and **Ebrahim, 2010**. A variety of physicochemical mechanisms/forces, such as van der Waals, ion exchange, dipole interactions, H-binding, cation bridging, covalent bonding, and water bridging, can be responsible for the biosorption of inorganic compounds in biomass. **Sulaymon et al., 2012**. Metal uptake is caused by physico-chemical interaction between the metal and the functional groups present on the microbial cell surface, which is not dependent on the cells' metabolism **Vijayaraghavan** and **Yun, 2008**. Cell walls of microbial biomass, mainly composed of polysaccharides, proteins and lipids have abundant metal binding groups such as carboxyl, sulphate, phosphate and amino groups. This type of biosorption, i.e., non-metabolism dependent is relatively rapid and can be reversible **Sulaymon et al., 2012 b**.

Fixed bed adsorber is a continuous flow operation adsorption process for industrial applications in wastewater treatment **Ahmed, 2006**. The design of an adsorption column depends on various important parameters such as flow rate, initial concentration and bed height (mass of biomass). The sorption bed has to be porous to allow the liquid to flow through it with minimum resistance but allowing the maximum mass transfer into the particles as small as practical 0.7-1.5 mm **Sulaymon et al., 2012 b** Understanding of biosorption characteristics, determination of break point time for biosorption operation and effective utilization of the column is possible by carrying out the mathematical modeling of fixed-bed biosorption columns. Continuous biosorption studies are required to collect the experimental data for the design of biosorption column and for subsequent scale-up from pilot plant to industrial scale operation **Ahmed, 2006**. Past studies mainly focused on

analytical approach of solving the dynamics of fixed-bed adsorption columns. These models, exclude some of the important physical aspects such as axial dispersion and intra-particle resistances along the bed length and linear isotherm such as: second-order reversible reaction model (SRRM) and quasichemical kinetic model (QKM) and homogenous surface diffusion model (HSDM) described by **Pérez et al.,2013**. In the present study, a general multi-component model is used to predict the breakthrough curves of metal ions mixture in fixed bed column for single and binary components onto DAB and compare the experimental results with that simulated by a numerical solution of the model which includes film mass transfer, pore diffusion resistance, axial dispersion and nonlinear isotherm **Sulaymon et al., 2012 a**.

2. MATHEMATICAL MODELING AND SIMULATION

In the present study, a mathematical model for the fixed bed column is proposed by incorporation of important parameters such as external mass transfer resistance, internal mass transfer resistance and nonlinear multi-component isotherm **Ahmed, 2006**. The proposed model can be extensively used for understanding the dynamics of the fixed bed adsorption column for the biosorption of multi-inorganic (metal ions) compounds. To formulate a generalized model for the fixed bed adsorption column, the following assumptions are made **Sulaymon et al., 2012 a**:

- Equilibrium of adsorption is described by the nonlinear multi-component Langmuir isotherm.
- Mass transfer across the boundary layer surrounding the solid particles is characterized by external-film mass transfer coefficient (k_f).
- Intra-particle mass transfer is characterized by pore diffusion coefficient (D_p)
- Macro-porous adsorbent particles are spherical and homogeneous in size and density.
- Compressibility of the mobile phase is negligible.
- Fluid inside particles (macropores) is stagnant, i.e., there is no convective flow inside macropores.
- The adsorption process is isothermal. There is no temperature change during a run.
- The concentration gradients in the radial direction are negligible.
- All mechanisms which contribute to axial mixing are lumped together into a single axial dispersion coefficient.

Based on the assumptions of the model, the governing equations for a multi-component system can be obtained from differential mass balance of the bulk-fluid phase and the particles phase respectively:

Continuity equation in the bulk-fluid phase Eq.(1):

$$-D_{bi}\frac{\partial^2 C_{bi}}{\partial Z^2}+V_i\frac{\partial C_{bi}}{\partial Z}+\frac{\partial C_{bi}}{\partial t}+\frac{3k_{fi}\left(1-\varepsilon_b\right)}{\varepsilon_b R_p}\left[C_{bi}-C_{pi,R=R_p}\right]=0 \quad (1)$$

Continuity equation inside the particle phase Eq.(2):

$$\left(1-\varepsilon_p\right)\frac{\partial C_{pi}^{*}}{\partial t}+\varepsilon_p\frac{\partial C_{pi}}{\partial t}-\varepsilon_p D_{pi}\left[\frac{1}{R_p^2}\frac{\partial}{\partial R_p}\left(R_p^2\frac{\partial C_{pi}}{\partial R_p}\right)\right]=0 \quad (2)$$

Initial and Boundary Conditions:
The initial and boundary conditions may be represented by Eq.(3) to Eq.(8):

Initial Condition (t = 0):

$$C_{bi}=C_{bi}(0,Z)=0 \quad (3)$$

$$C_{pi}=C_{pi}(0,R,Z)=0 \quad (4)$$

Boundary Conditions:
Z = 0:

$$\frac{\partial C_{bi}}{\partial Z}=\frac{\nu}{D_{bi}}\left(C_{bi}-C_{oi}\right) \quad (5)$$

Z =L:

$$\frac{\partial C_{bi}}{\partial Z}=0 \quad (6)$$

R = 0:

$$\frac{\partial C_{pi}}{\partial R}=0 \quad (7)$$

$R = R_p$:

$$\frac{\partial C_{pi}}{\partial R}=\frac{k_{fi}}{\varepsilon_p D_{pi}}\left(C_{bi}-C_{pi,R=R_p}\right) \quad (8)$$

Dimensionless Groups:
Defining the following dimensionless variables:

$$c_{bi}=\frac{C_{bi}}{C_{oi}},\ c_{pi}=\frac{C_{pi}}{C_{oi}},\ c_{pi}^{*}=\frac{C_{pi}^{*}}{C_{oi}},\ \tau=\frac{\nu t}{L},\ r=\frac{R}{R_p},\ z=\frac{Z}{L}$$

Also, the dimensionless parameters are defining as:

$$Pe_i = \frac{vL}{D_{bi}},\ Bi_i = \frac{k_{fi}R_p}{\varepsilon_p D_{pi}},\ \eta_i = \frac{\varepsilon_p D_{pi} L}{R_p^2 v},\ \zeta_i = \frac{3Bi_i\eta_i(1-\varepsilon_b)}{\varepsilon_b}$$

The model equations can be transformed into the following dimensionless Eq. (9) and Eq.(10):

$$-\frac{1}{Pe_i}\frac{\partial^2 c_{bi}}{\partial z^2} + \frac{\partial c_{bi}}{\partial z} + \frac{\partial c_{bi}}{\partial \tau} + \zeta_i\left(c_{bi} - c_{pi,r=1}\right) = 0 \quad (9)$$

$$\frac{\partial}{\partial \tau}\left[\left(1-\varepsilon_p\right)c_{pi}^{*} + \varepsilon_p c_{pi}\right] - \eta_i\left[\frac{1}{r^2}\frac{\partial}{\partial r}\left(r^2\frac{\partial c_{pi}}{\partial r}\right)\right] = 0 \quad (10)$$

In these equations, the Peclet number (Pe_i) reflects the ratio of the convection rate to the dispersion rate, while the Biot number (Bi_i) reflects the ratio of the external film mass transfer rate to the intra-particle diffusion rate.
Initial conditions become ($\tau = 0$) **Ahmed, 2006** Eq.(11) and Eq.(12):

$$c_{bi} = c_{bi}(0, z) = 0 \quad (11)$$

$$c_{pi} = c_{pi}(0, r, z) = 0 \quad (12)$$

And boundary conditions become Eq(15) to Eq(16);

z = 0: $$\frac{\partial c_{bi}}{\partial z} = Pe_i\left(c_{bi} - 1\right) \quad (13)$$

z =1: $$\frac{\partial c_{bi}}{\partial z} = 0 \quad (14)$$

r = 0:

$$\frac{\partial c_{pi}}{\partial r} = 0 \quad (15)$$

r = 1:

$$\frac{\partial c_{pi}}{\partial r} = Bi_i\left(c_{bi} - c_{pi,r=1}\right) \quad (16)$$

The concentration c_{pi}* in Eq.(10) is the dimensionless concentration of component *i* in the solid phase of the particles. It is directly linked to a multi-component isotherm, which is the extended Langmuir model Eq.(17) and Eq.(18):

$$C_{pi}^{*}=\frac{q_{mi}\rho_p b_i C_{pi}}{1+\sum_{j=1}^{N_s} b_j C_{pj}}=\frac{\rho_p a_i C_{pi}}{1+\sum_{j=1}^{N_s} b_j C_{pj}} \quad (17)$$

And in dimensionless form:

$$c_{pi}^{*}=\frac{\rho_p a_i c_{pi}}{1+\sum_{j=1}^{N_s}\left(b_j C_{oj}\right)c_{pj}} \quad (18)$$

Because of nonlinear multi-component Langmuir isotherm is considered, finite element method (Galerkin weighted residual method) is used for the discretization of the bulk-fluid phase partial differential equation and the orthogonal collocation method for the particle phase equation is produced. The ordinary differential equation system with initial values can be readily solved using an ordinary differential equation solver such as the subroutine "ODE15S" of MATLAB V-7.3 which is a variable order solver based on the numerical differentiation formulas (NDFs**) Sulaymon** and **Ahmed, 2008**.

3 EXPERIMENTAL MATERIALS AND PROCEDURE

3.1 Adsorbate

Standard stock solutions of 1000 mg/l of lead (II) and chromium (III) were prepared by dissolving $Pb(NO_3)_2$ and $Cr(NO_3)_3$ (BDH, England with minimum purity 99.5 %). The salts obtained from a local market with specifications are shown in **Table1**. Lead nitrate of 0.1599 g and 4.577 g of chromium nitrate were dissolved in 1 L distilled water. Metal concentrations were determined by a flame atomic absorption spectrophotometer Buck, Accusys 211, USA

3.2 Adsorbent

Heterogeneous cultures including mostly anaerobic bacteria, yeast fungi and protozoa of sorbents were taken from Al-Rustomia third extension drying bed Baghdad-Iraq. The physical, chemical and biological properties were measured and listed in **Table 2**. Anaerobic and facultative anaerobic microorganisms (*Aeromonas species, E-coli, Pseudomonas aerginrsa, Clostridium, Staphylococcus sp and Salmonella sp, Rhizopusarrhizus, Saccharomyces erevisiae)* were found in the biomass from the drying beds using API Instrument (Biomerieux, France). Preparation (DAB) using heterogeneous culture of live anaerobic biomass (LAB) was dried at temperature (37-45°C) for 5 days crushed, sieved, washed with distilled water and dried at 70°C for 6 h.

3.3 Procedure

Solutions pH were adjusted to the desired value (pH=4) using 0.1 M NaOH or 0.1 M HNO_3. With pH higher than 5.5, solubility of metal complexes decreases sufficiently allowing precipitation, which may complicate the sorption process and do not bind to the adsorption sites on the surface of DAB. These flasks were then placed on a shaker (HV-2 ORBTAL, Germany) and agitated continuously for 4 h at 200 rpm and (33±3°C). The samples were filtered by no. 42

Whatman filter paper. Few drops of 0.1 M HNO_3were added to the samples to decrease the pH below 2 in order to fix the concentration of the heavy metals during storage before analysis **APHA, 1995**.The final equilibrium concentrations were measured by means of atomic absorption

The fixed bed adsorber was made of an acrylic column of 0.05 m inner diameter and 0.5 m height **Fig. 1**. The DAB bed is confined in the column by fine stainless steel screen and glass cylindrical packing at the bottom and also at the top of the bed to ensure a uniform distribution of influent through the biomass bed. A perforated plate is fixed at the top of the column where the influent solution is introduced to the column.
For determination of the biosorption isotherm, different weights (0.05, 0.1, 0.15… to 0.6 g) of dry dead anaerobic biomass were used, (electronic balance Sartorius BL 210S); biosorbent were placed in 12 volumetric flasks of 250 mL. A volume of 100 mL of solution with concentration of 50 mg/L was added to each flask for single systems of Pb(II), Cr(III) ions respectively. The experiment was performed at sufficiently high metal concentrations so that maximal uptake would be achieved. The adsorbed amount was calculated using Eq. (19) **Sulaymon et al., 2012 b**

$$q_e = \frac{V_L(C_o - C_e)}{W_A} \tag{19}$$

The necessary dosage of DAB used for kinetic study, to reach equilibrium related concentration of C_e/C_o equal to 0.05, were calculated from Langmuir isotherm model and mass balance equation Eq.(20) With Eq.(21)

$$W_A = \frac{V_L(C_o - C_e)}{q_e} \tag{20}$$

$$q_e = \frac{q_m b C_e}{1 + b C_e} \tag{21}$$

The important characteristic of the Langmuir isotherm can be expressed in terms of the dimensionless constant separation factor for equilibrium parameter R_L. This is defined by:

$$R_L = \frac{1}{1 + b\mathrm{C_e}} \tag{22}$$

The adsorption isotherms were obtained by plotting the weight of solute adsorbed per unit weight of biomass q_e, mg/g against the equilibrium concentration of the solute in the solution C_e, mg/L, and R_L Separation factor Eq. (22) **Sulaymon** and **Ebrahim 2010**. Reaction pathways were found using 2L pyrex beaker fitted with variable speed mixer. The beaker was filled with 1 L of 50 mg/L concentration and the agitation started before adding value of DAB. At time zero, the accurate weight of DAB where added and samples were taken at specified time intervals. Pore diffusion coefficient (D_p) of Pb(II) and Cr(III) was obtained using a batch model by matching the concentration decay curve obtained from the experimental data. At the beginning the pore diffusion coefficient is assumed and the model is solved numerically using MATLAB program. This process continued until obtaining perfect matching between the theoretical and experimental concentration

decay curve. The principle parameter required for solving the batch model is the external mass transfer coefficient (k_f) Eq.(23) and the assumed pore diffusion coefficient (D_p). Eq.(24) The external mass transfer coefficient kf and Molecular diffusivity D_m in the fixed bed column model were calculated using the correlation of Crittenden Eq.(25) **Sulaymon** and **Ahmed, 2008**.

$$k_f=2.4V_s/(Sc^{0.58}\,R_e^{0.66}) \quad (23)$$

The liquid diffusivity coefficient was calculated using Eq.(24):

$$D_m=2.74*10^{-9}\,(MW)^{-1/3} \quad (24)$$

The axial dispersion coefficient D_b of the liquid flowing through fixed beds was obtained from the following correlation **Urban** and **Gomezplata, 2009**:

$$\frac{D_z}{D_m}=0.67+1.15\left[\frac{V_s d_p}{D_m}\right]^{1.2} \quad (25)$$

4 RESULTS AND DISCUSSION

4.1 Adsorption Isotherm

The equilibrium isotherm for the investigated solutes (Pb^{+2} and Cr^{+3}) onto DAB using multi-component Langmuir model are presented in **Fig.2**. The correlation coefficient (R^2) between the experimental data and the theoretical model is 0.958 and 0.999 for lead and chromium respectively. The Langmuir parameters are as follows:

- Pb^{2+}: q_m= 35.12 mg g^{-1}, b= 0.311 L mg^{-1}, R^2 = 0.958
- Cr^{+3}: q_m= 23.84 mg g^{-1}, b= 0.165 L mg^{-1}, R^2 = 0.999

To compare these results obtained by DAB with other absorbents, **Table 3** comparison of metal adsorption capacities (mg/g) onto different adsorbents

4.2 Pore Diffusion Coefficient

Pore diffusion coefficients (D_p) of chromium and lead are obtained using the batch model by matching the concentration decay curve obtained from the experimental data at optimum agitation speed 400 rpm with that obtained from the batch model as shown in **Fig. 3**. The pore diffusion coefficients for each solute are evaluated from batch experiments to be:

- Pb^{2+}: $D_p = 7.23\times10^{-11}$ m^2s^{-1}, R^2 = 0.994
- Cr^{+3}: $D_p = 3.15\times10^{-11}$ m^2s^{-1}, R^2 = 0.971

With $k_f=4.73\times10^{-5}$ m/s for Pb^{+2} and $k_f=2.4\times10^{-5}$ m/s for Cr^{+3}

4.3 Breakthrough Curves of The Binary System

The experimental and predicted breakthrough curves for single and binary systems for adsorption of lead and chromium ions onto DAB at different flow rates, bed height and initial concentration are shown in **Figs. 4 to 8**.

5 DISCUSSION

1. The adsorption capacity order for lead and chromium onto DAB was as follow:
Pb^{+2} (35.12 mg g^{-1}) > Cr^{+3} (23.84 mg g^{-1}). This behavior of the capacity of the adsorbate in batch system seems to influence the adsorption capacity of DAB in fixed bed adsorber. This can be explained by:

a- Lead nitrate has less solubility (520000 mg L^{-1}) in water in comparison with chromium nitrate (810000 mg L^{-1}).
b- Hydrated ion radius for lead is greater than chromium (4.01 $Å^2$ for lead and 4.13 $Å^2$ for chromium).
c- Lead can be adsorbed by means of electrostatic attraction between positively charged and binding sites. Physical adsorption by means of Vander Waals, and dipole-induced dipole has been the main way to adsorb lead ions with high electronegativity (2.33) in comparison with chromium (1.66) **Table 1**. However, lead and chromium ions biosorption depended on the activity and availability of functional groups onto DAB (electrostatic attraction) with the mean of competitive biosorption **Sulaymon et al, 2012 b**.

2. The effect of flow rate:

Figs.4,5 and 6 shows the experimental and predicted breakthrough curves for Pb^{+2} and Cr^{+3} in single and binary systems at different flow rates (1.39×10^{-6}, 2.78×10^{-6}, 4.17×10^{-6} $m^3s^{-1}$and 5.56×10^{-6} m^3s^{-1}) in terms of C_e/C_o. It's clear from these figures that as the flow rate increases, the time of breakthrough point decreases. This is because that the residence time of solute in the bed decreases. Therefore there is not enough time for adsorption equilibrium to be reached which results in lower bed utilization and the adsorbate solution leaves the column before equilibrium. It is expected that the change in flow rate will affect the film diffusion but not the intra-particle **diffusion Sulaymon** and **Ahmed, 2008**. The higher the flow rates, the smaller film resistance to mass transfer and hence larger k_f results. Increasing the flow rate at constant bed height will increase the Bi number with slight increase in Pe number as listed in **Table 4**. When the Bi number is high the time of breakthrough point will appear early. The higher Bi number values indicate that the film diffusion is not dominating compared to the intra-particle mass transfer and the intra-particle mass transfer is the controlling parameter **Fig. 6**. These results agree with those obtained by **Sulaymon et al.,2012 .**

3. Effects of bed height:

Fig. 8 shows that at smaller bed height the effluent adsorbate concentration ratio increases more rapidly than that for a higher bed height. Furthermore, smaller bed heights will be saturated in less time. Smaller bed heights corresponds to lesser amount of adsorbent, at a given flow rate and increasing the bed height will increase the contact time of the solute within the bed, thus improving the three solute removal efficiencies

Increasing the bed height at constant flow rate will increase Peclet number (Pe). Pe is the ratio of axial convection rate to axial dispersion rate. When Pe is small the breakpoint appears early and the breakpoint increases with increasing Pe as listed in **Table 4**. Therefore both the internal and external resistances are considered as the major items controlling the adsorption kinetics as the bed height increases. A deep bed requires more time to reach saturation point or a breakpoint appearing later. Also, larger bed provide greater surface area or (adsorption sites) which causes increasing adsorption process and contact time. The bed height is one of the major parameters in the design of

fixed bed adsorption column **Sulaymon et al., 2012 a**. The experimental and predicted breakthrough curves obtained for different heights of DAB 0.05, 0.1, 0.15 and 0.2 m at constant flow rate and constant initial concentration are presented in **Fig.8**. Hence, the internal and external resistances are confirmed to be the main parameters that control the adsorption kinetics with the increase in bed height. Similar findings have been obtained by **Sulymoon et al., 2012 a**

4. Effect of initial concentration:

The change in initial concentrations of Pb^{+2} and Cr^{+3} will have a significant effect on the breakthrough curves. **Fig.7** shows the experimental and predicted breakthrough curves at different initial concentrations (25, 50, 75 and 100 mg L^{-1}). This figure shows that an increase in initial concentration causes a decrease in breakpoint time and makes the breakthrough curves much steeper, this would be anticipated with the basis of increasing driving forces for mass transfer with increasing the concentration of solutes. As the initial concentration increases the time of breakthrough point decreases. This may attribute to the diffusion rate and controlled by the concentration gradient, it will take a longer time to reach saturation in the case of low initial solute concentration. It is also clear that as the influent concentration increases, the adsorption capacity increases. These results are in agreement with that obtained by **Sulaymon** and **Ahmed, 2008**.

5. In multi-component system (binary system) for lead and chromium, it is clear from **Figs. 6,7**, and 8 that, at the initial stage, there are a lot of active sites of DAB, and the strongly (Pb^{+2}) and weakly (Cr^{+3}) adsorbed component take the active site freely. With increasing time, the weakly adsorbed component is not easily adsorbed but moves ahead with the bulk-fluid and the strongly adsorbed component tends to displace the sites that had been taken by the weakly adsorbed component. The result is that the local concentration of the weakly adsorbed component within the fixed bed adsorber is higher. These results are in agreement with that obtained by **Sulaymon et al., 2012 a.**

6 CONCLUSIONS

The simulated breakthrough curves for adsorption of lead and chromium both in single and binary systems onto dead anaerobic biomass are in close agreement with the experimental results. Thus, the mathematical model, which includes axial dispersion, film mass transfer, pore diffusion resistance and nonlinear isotherm, provides a good description of the single and competitive adsorption process in fixed bed adsorbed. As the flow rate increases, the Biot number arranges to for Pb(II) ions from 74.6 to 119, for Cr(III) ions from 155 to 249 for each solute, the rate of competitive adsorption will decrease and the shape of breakthrough curves will be sharp with lower breakpoint, due to the high intra-particle resistance and the decrease in contact time to reach saturation. Finally DAB was found to be more suitable adsorbent for removal of lead than chromium the same conclusions were obtain by **Sulaymon et al., 2012 a.**

REFERENCES

Ahmed, K. W., 2006, *Removal of Multi-pollutants from Wastewater by Adsorption Method*, Ph.D. Thesis, University of Baghdad

APHA, 1995, *Sta*ndard *Methods for the Examination of Water and Wastewater*, 19th edn. American Public Health Association,Washington, DC.

Fiol, N., Poch J., and Villaescusa I., 2004, *Chromium (VI) Uptake by Grape Stalks wastes Encapsulated in Calcium Alginate Beads: Equilibrium and Kinetics Studies*, Chemical Speciation and Bioavailability Vol.16, No.2, PP. 25-33.

Gupta, V. K., and Ali, I. 2004 *Removal of Lead and Chromium from Wastewater using Bagasse Fly Ash - A Sugar Industry Waste*. Journal of Colloid Interface, Vol.271, PP. 321-328.

Gupta, V. K., and Rastogi, A., 2009 *Biosoprtion of Hexavalent Chromium by Raw and Acid-Treated Green Alga Oedogonium Hatei from Aqueous Solutions*, Journal of Hazardous Materials, Vol. 163, PP. 396- 402.

Huifen, L., Yanbing, L., Wumeng, G., Jiali, C., Lin, X., and Junkang, G,. 2010, *Biosorption of Zn(II) by Live and Dead Cells of Streptomyces Ciscaucasicus Strain CCNWHX 72-14*. Journal of Hazardous Materials, Vol.179, PP. 151–159.

Lawrence, K., Wang, J. T., Stephen, T. T., and Yung, T., H., 2010, *Handbook of Environmental Engineering, Environmental Bioengineering*. Springer New York Dordrecht Heidelberg London.

Naseem, R., and Tahir, S., S., 2001, *Removal of Pb(II) from Aqueous Solution By using Bentonite as an Adsorbent*. Journal of Water Research, Vol. 35, PP. 3982 – 3986.

Pérez, F., A., Casoni, E., and Huerta A., 2013, *Dimensionless Analysis of HSDM and Application to Simulation of Breakthrough Curves of Highly Adsorbent Porous Media*, Journal of Environmental Engineering, Vol. 139, No.5, PP. 667–676.

Prasad, M., Xu, H., Y., and Saxena, S., 2008, *Multi-Component Sorption Of Pb(II), Cu(II) and Zn(II) Onto Low-Cost Mineral Adsorbent,* Journal of Hazardous Materials, Vol. 154, PP. 221 – 229.

Sekomo, C. B., Kagisha, V., Rousseau, D., P., and Lens, P., N., 2011, *Heavy Metal Removal by Combining Anaerobic Upflow Packed Bed Reactors with Water Hyacinth Ponds*. Environmental Technology, Vol. 32, No.1, PP.87-95.

Sulaymon, A., H., Abbood, D., W., and Ali, A., H., 2012 a, *Removal of Phenol and Lead from Synthetic Wastewater by Adsorption onto Granular Activated Carbon in Fixed Bed Adsorbers: Prediction of Breakthrough Curves*, Desalination and Water Treatment, Vol.40, No.1-3, PP. 244-253.

Sulaymon, A., H., and Ahmed, K., W., 2008, *Competitive Adsorption of Furfural and Phenolic Compounds onto Activated Carbon in Fixed Bed Column,* Environmental Science Technology, Vol. 42, No.2, PP.392-7.

Sulaymon, A., H., and Ebrahim, S., E., 2010, *Removal of lead, cadmium, and mercury ions using biosorption*, Desalination Water Treatment, Vol. 24, PP.44–352.

Sulaymon, A., H., Ebrahim, S., E., and Ridha, M., J., 2012 b, *Equilibrium, kinetic, and thermodynamic biosorption of Pb(II), Cr(III), and Cd(II) ions by dead anaerobic biomass from synthetic wastewater*, Environmental Sciences Pollution Research, Vol. 20, No.1, PP.75-187.

Tuzun, I., Bayramoglu, G., Alcin, Y., E., Basaran, G., Celik, G., and Arica, M., Y., 2005, *Equilibrium and kinetic studies on biosorption of Hg(II), Cd(II) and Pb(II) ions onto microalgae Chlamydomonas reinhardtii*. Journal Environmental Management, Vol.77, PP. 85-92.

Urban, C., and Gomezplata, A., 2009, *Axial Dispersion Coefficients in Packed Beds at Low Reynolds Numbers*, The Canadian Journal of Chemical Engineering, Vol. 47, No. 4, PP.353–359.

Van-Hullebusch, E., D., Gieteling, J., Zhang, M., Zandvoort, M., H., Daele, W., V., Defrancq, J., and Lens, P., N., L., 2006, *Cobalt sorption onto anaerobic granular sludge: isotherm and spatial localization analysis,* Journal of Biotechnology, Vol. 121, No. 2, PP. 227 – 240.

Vijayaraghavan K., and Yun, Y-S., 2008, *Bacterial biosorbents and biosorption*, Biotechnology Advance, Vol. 26, PP.266–291.

NOMENCLATURE

Å	Angstrom, 1×10^{-10} m
b	Adsorption equilibrium constant relate to affinity between adsorbent and adsorbate, L mg^{-1}
Bi	Biot number
C	Fluid phase concentration, mg L^{-1}
C_e	Equilibrium liquid phase concentration, mg L^{-1}
C_o	Initial liquid phase concentration, mg L^{-1}
D_b	Axial dispersion coefficient m^2/s
D_m	Molecular diffusivity, m^2 s^{-1}
D_p	Pore diffusion coefficient, m^2 s^{-1}
d_p	Particle diameter, m
k_f	External mass transfer coefficient, m s^{-1}
MW	Molecular weight, g mol^{-1}
L	Length of the column, m
P_e	Peclet number
Q	Flow rate, m^3 s^{-1}
q_e	Adorption capacity at equilibrium, mg g^{-1}
q_m	Langmuir constant related to maximum adsorption capacity, mg g^{-1}
r	Radial coordinate, m
R	Radial coordinate, m
Re	Renold number,$Re=\rho_w \upsilon d_p/\mu_w$
R_p	Radius of particle, m
Sc	Schmidt number, $Sc= \mu_w/\rho_w D_m$
Sh	Sherwood number, $Sh=k_f d_p/D_m$
t	Time, s
V_L	Volume of solution, L

W_A	Mass of dead anaerobic biomass, g	i	Component number, 1,2,…
		L	Liquid Phase
Z	Axial distance, m	o	Initial phase
ε_b	Bed porosity	p	Particle phase
ε_p	Particle porosity	Cr^{3+}	Chromium
μ_w	Viscosity of water	Pb^{2+}	Lead
υ	Interstitial velocity, $\upsilon=Q/\pi R^2{}_p\varepsilon_b$		
ρ_w	Density of water, kg/m^3		
ρ_p	Particle density, kg/m^3		
Subscript			
b	Bulk fluid phase		
e	Equilibrium		
DAB	Dead anaerobic biomass		

Table 1. Main physicochemical properties of the metals tested.

Properties	Lead	Chromium
Formula	Pb(II) from $Pb(NO_3)_2$	Cr(III) from Cr $(NO_3)_3$
Appearance	White colorless crystals	blue-violet crystals
Molar mass, g/mole	331.2	238.011
Standard atomic weight	207.2	51.99
Solubility in water, g/100 mL	52	81
Molecular diffusion, $m^2/s\times10^{-8}$	4.98	4.22
Hydrated ion radius (Å)	4.01	4.13
Crystal radius (Å)	1.19	0.75
Electronegativity	2.33	1.66
Charge	2	3
Density, g/cm^3	4.53	1.85
Wavelengths used by AA, nm	283.3	357.9
Company	BDH (England)	BDH (England)

Table 2. Physical chemical and biological characteristic of DAB.

Biomass			
Physical characteristic (dead biomass)		Biological characteristic (live biomass)	
Particle diameter, mm	0.775	*Bacteria*	
Surface area, m^2/g	94.53[(a)]	*Aeromonas species, CFU/mL*	222000
Actual density, kg/m	1741.6	*E-coli, CFU/mL*	430000
Bulk density, kg/m	609.9[(b)]	*Pseudomonas aerginrsa, CFU/mL*	703500
Particle porosity	0.584	*Klebsiella species, CFU/mL*	210000
Total Suspended Solid, mg/L	153950	*Clostridium, CFU/mL*	370000
Volatile Suspended, mg/L	78126	*Staphylococcus sp., CFU/mL*	210000
Chemical characteristic (dead biomass)		*Streptococcus sp., CFU/mL*	490000
pH	5.5-6.3	*Salmonella sp., CFU/mL*	190000
CEC, meq/100g	51.2	*Shiglla dysente, CFU/mL*	410000
Lead, mg/L	0. 02	*Fungi*	
Chromium, mg/L	0.01	*Penicillium sp., CFU/mL*	180000
Cadmium, mg/L	0.02	*Yeast*	
		Candida albicans, CFU/mL	460000
		Protozoa	
		Entamoeba species, CFU/mL	16000
		Giardia lambihia, CFU/mL	90000

(a) Surface area analyzer, BET method, Quantachrome.com.(USA), (b) Apparent density instrument, Autotap, Quantachrome.(USA), CEC Cat ion Exchange Capacity, CFU Colony-forming unit

Table 3. Comparison of metal adsorption capacities (mg/g) onto different adsorbents.

Adsorbent	pH	Other information	Pb(II)	Cr(III)	Reference
Granular Activated Carbon	7.5	M=30 g/L, t_{eq}= 30 h	45(L)	23(L)	Lawrence et al. 2010
Waste sorbent Sugar beet pulp	5.5	M=1 g/L, t_{eq}= 8 h	74(E)	36(E)	Lawrence et al. 2010
bagasse fly ash	5-6	M=10 g/L,	3.8(E)	1.8(E)	Gupta and Ali
		t_{eq}= 1 h			2004
Green algae *Spirogyra sp.*	5	M=10 g/L, t_{eq}= 1.8 h	93.5(E)	----	Gupta and Rastogi 2009
Fungus *Sargassum natans*	3.5	M=1 g/L, t_{eq}= 1 h	252.5(L)	----	Huifen et al. 2010
Macrolagae Chlamydomonas reinhardtii	5	M=1 g/L, t_{eq}= 24 h	24.9 (L)	----	Tuzun et al. 2005
This study (binary system)	4	M=0.5 g/L, t_{eq} = 4 h	35.12 (E)	23.84 (E)	

E Experimental uptake, L uptake predicted by the Langmuir model, M biosorbent dosage, t_{eq} equilibrium time, ----- not available

Table 4. Values of Biot no. and Peclet no. at different flow rates and bed heights.

Pollutants	Flow rate,m^3s^{-1}	Biot no. (Bi)	Peclet no.(Pe)	Bed height, m	Biot no. (Bi)	Peclet no.(Pe)
Pb^{+2}	1.39×10^{-6}	74.6	131	0.05	74.6	32.7
	2.78×10^{-6}	93.3	134	0.10	74.6	65.4
	4.17×10^{-6}	108	137	0.15	74.6	98.0
	5.56×10^{-6}	119	139	0.20	74.6	131
Cr^{+3}	1.39×10^{-6}	115	131	0.05	155	32.7
	2.78×10^{-6}	197	134	0.10	155	65.4
	4.17×10^{-6}	226	137	0.15	155	98.0
	5.56×10^{-6}	249	139	0.20	155	131

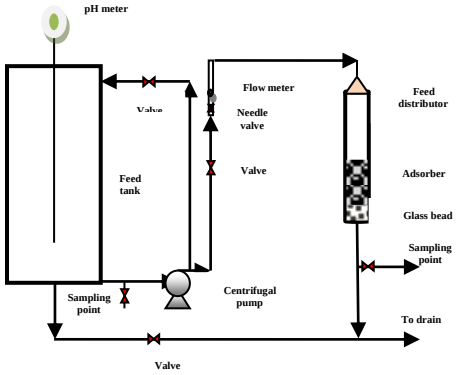

Figure1. Fixed bed biosorption column.

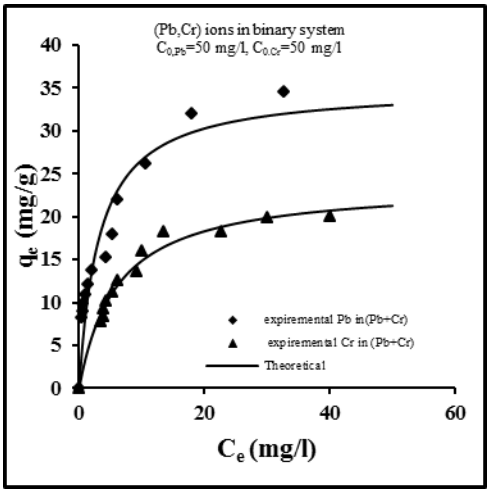

Figure 2. Biosorption isotherm for (Pb^{+2}, Cr^{+3}) onto DAB**.**

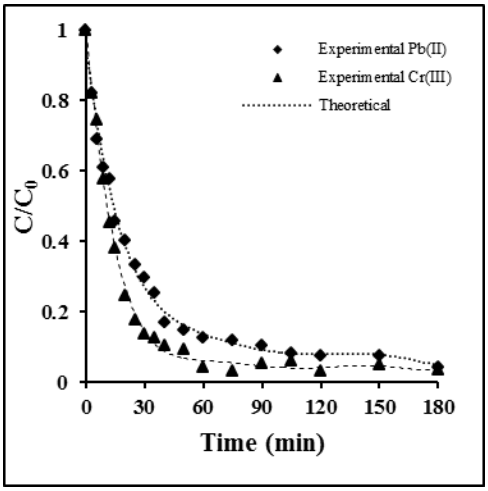

Figure 3. Comparison of the measured concentration-time decay data with that predicated by pore diffusion model for Pb^{+2} and Cr^{+3}. $k_f=4.73\times10^{-5}$ m/s for Pb^{+2} and $k_f=2.4\times10^{-5}$ m/s for $Cr^{+3.}$

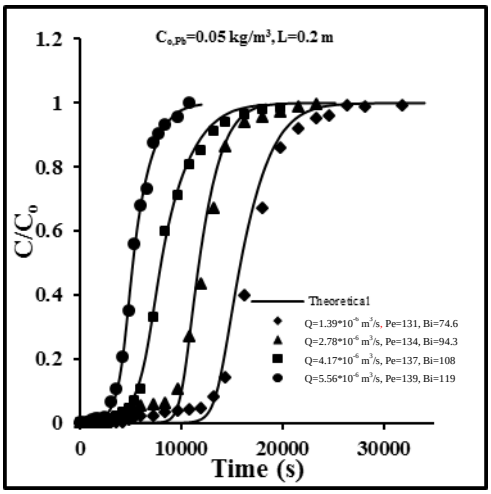

Figure 4. Experimental and predicted breakthrough curves for biosorption of lead onto DAB at different flow rate.

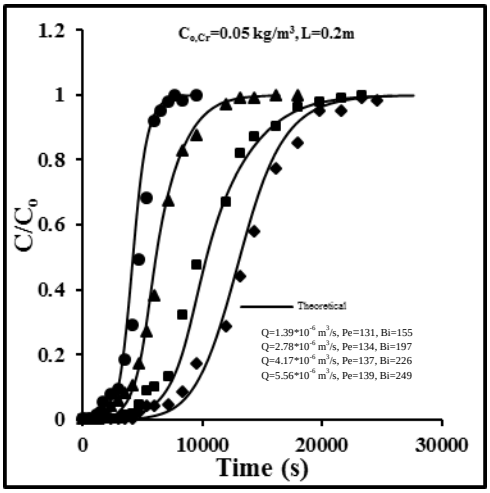

Figure 5. Experimental and predicted breakthrough curves for biosorption of chromium onto DAB at different flow rates.

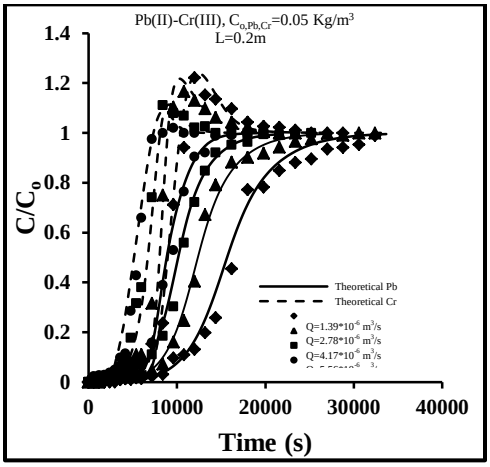

Figure 6. Experimental and predicted breakthrough curves for biosorption of Pb(II)-Cr(III) system onto DAB at different flow rates.

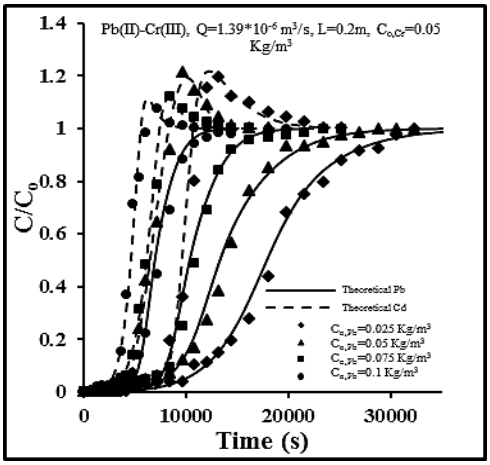

Figure 7. Experimental and predicted breakthrough curves for biosorption of Pb(II)-Cd(II) system onto DAB at different initial concentrations of Pb(II) ions.

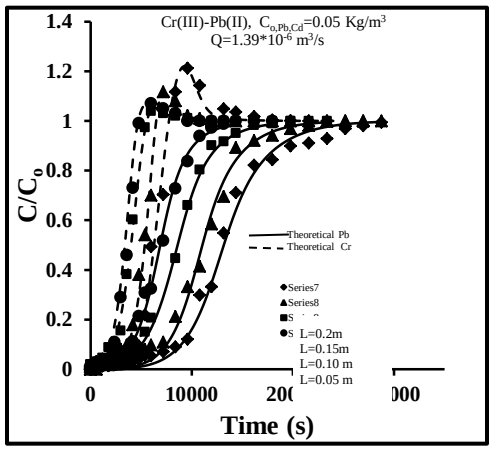

Figure 8. Experimental and predicted breakthrough curves for biosorption of Cr(III)-Pb(II) system onto DAB at different bed heights.